OBSERVATIONS OF THE CIRCUMSTELLAR WATER $1_{10} \rightarrow 1_{01}$ AND AMMONIA $1_0 \rightarrow 0_0$ LINES IN IRC +10216 BY THE *ODIN* SATELLITE

T. I. HASEGAWA,[1] S. KWOK,[1] N. KONING, AND K. VOLK[2]

Department of Physics and Astronomy, University of Calgary, Calgary, Alberta T2N 1N4, Canada; hasegawa@iras.ucalgary.ca, kwok@iras.ucalgary.ca, nkoning@iras.ucalgary.ca

K. JUSTTANONT, H. OLOFSSON, F. L. SCHÖIER, AND AA. SANDQVIST

Stockholm Observatory, AlbaNova, SE-106 91 Stockholm, Sweden

Å. HJALMARSON, M. OLBERG, AND A. WINNBERG

Onsala Space Observatory, S-43992 Onsala, Sweden

L.-Å. NYMAN

European Southern Observatory, Alonso de Cordova 3107, Vitacura, Casilla 19001, Santiago, Chile

AND

U. FRISK

Swedish Space Corporation, Box 802, SE-981 28 Kiruna, Sweden

ABSTRACT

Submillimeter lines of H_2O and NH_3 have been detected in the carbon star IRC +10216 (CW Leo) with the *Odin* submillimeter satellite. The detection of the $J_{K^-,K^+} = 1_{10} \rightarrow 1_{01}$ 557 GHz line of ortho-H_2O confirms the earlier detection in the same source with *SWAS*. The detection of the $J_K = 1_0 \rightarrow 0_0$ 572 GHz line represents the first observation of the ground-state rotational transition of NH_3 in a stellar envelope. By fitting a molecular line transfer model to the observed lines, we derive an ortho-H_2O abundance of 2.4×10^{-6}, which is consistent with estimates from the *SWAS* observation. The derived ortho-NH_3 abundance of 1×10^{-6} relative to H_2 is significantly higher than those derived from 24 GHz inversion transitions and is slightly higher than those from vibrational transitions in the infrared band. The high H_2O and NH_3 abundances in the carbon-rich star IRC +10216 underscore shortcomings in the conventional gas-phase LTE and non-LTE chemical models.

Subject headings: circumstellar matter — molecular processes — stars: AGB and post-AGB — stars: individual (CW Leo)

1. INTRODUCTION

IRC +10216 (CW Leo) is a carbon-rich asymptotic giant branch (AGB) star that is undergoing extensive mass loss. The dust ejected by the star forms a thick circumstellar envelope (CSE) that obscures the photosphere of the star. Consequently, while it is very bright in the infrared, the star is very faint in the visible due to circumstellar extinction. The CSE is also a site of active chemistry, where more than 50 molecular species have been detected (Glassgold 1996; Olofsson 1999). The very high mass-loss rate inferred from the strengths of the molecular lines suggests that the star is rapidly depleting its hydrogen envelope and is about to leave the AGB to become a planetary nebula. The chemically rich molecular envelope makes IRC+10216 an ideal laboratory for the study of the formation mechanisms of molecules. Since the chemical timescale of molecular formation is limited by the dynamical time ($\sim10^4$ yr) of the stellar wind, the observations of molecular species give excellent constraints of chemical models.

Ammonia (NH_3) was first detected in IRC +10216 in the IR band in absorption of vibrational transitions by Betz et al. (1979). This IR detection was confirmed by Keady & Ridgway (1993), who derived an NH_3 abundance of 2×10^{-7} (relative to H_2), consistent with the earlier estimate by Betz et al. (1979). In a subsequent IR observation, Monnier et al. (2000) obtained a column density of NH_3 that is a factor of 4 higher than that by Keady & Ridgway (1993).

In the centimeter band, the 24 GHz inversion transition in the $J_K = 1_1$ rotational state of para-NH_3 has been detected in IRC +10216 (Kwok et al. 1981; Bell et al. 1982; Nguyen-Q-Rieu et al. 1984). From the strength of this inversion line, the inferred para-NH_3 to H_2 ratio is 3×10^{-8}. If the ortho/para NH_3 ratio is unity (a statistical equilibrium value in the high temperature limit), then the abundance from the inversion line is significantly lower than the values from vibrational transitions.

The surprising detections of NH_3 in the carbon star IRC +10216 have not drawn much attention. Detections of other more exotic molecules such as cyanopolyynes (e.g., HC_9N) and ring molecules (e.g., c-C_3H_2) probably overshadowed the significance of the NH_3 detections in IRC +10216. In fact, early thermochemical (LTE) models by Tsuji (1964) predicted very low abundances of NH_3 in carbon-rich stars. More recent studies of the LTE chemistry in carbon-rich stars (Cherchneff & Barker 1992; Lafont et al. 1982 and references therein) have only enforced the early prediction by Tsuji (1964), where the predicted NH_3/H_2 ratio is of order 10^{-12} or lower. The main reason for the low abundance of NH_3 in these models is because most of the nitrogen nuclei are tied up in HCN, CN, and N_2.

Non-LTE (gas-phase) chemical models for CSEs (IRC +10216, in particular) have been presented by many authors. However, NH_3 was not included in models by Glassgold et al. (1986), Cherchneff et al. (1993), or Glassgold (1996). Nejad &

Millar (1987) and Millar & Herbst (1994) assume a high abundance of NH_3 ($NH_3/H_2 = 2 \times 10^{-6}$) as an initial condition at the inner boundary of the model CSE, and the models show no net formation but only photodestruction of NH_3.

Willacy & Cherchneff (1998) included shock processing of ejected molecular gas in their models of IRC +10216, but the NH_3 abundance in their models only reaches 4×10^{-11} in the most favorable case. This discrepancy between theoretical and observational abundances of NH_3 (and CH_4 and SiH_4 as well) was pointed out by Willacy & Cherchneff (1998). This suggests that the conventional gas-phase chemistry models are inadequate, and grain-chemistry is probably needed to account for the observations (Willacy & Cherchneff 1998; Lafont et al. 1982; Keady & Ridgway 1993). The presence of NH_3 with rather high abundances in oxygen-rich stars is also a difficult problem (Menten & Alcolea 1995).

The infrared and microwave observations probe different excitation environments and have both advantages and drawbacks. In order to better determine the abundance of NH_3 and to further constrain theoretical models, it would be desirable to observe the lowest pure rotational transition $J_K = 1_0 \rightarrow 0_0$ of ortho-NH_3. In this paper, we report the observation of this 572 GHz transition in emission using the submillimeter-wave satellite *Odin*.

Water vapor was first detected in IRC+10216 by the *Submillimeter Wave Astronomy Satellite* (*SWAS*; Melnick et al. 2001). Since almost all chemical models predict that most elemental oxygen is tied up in CO in carbon-rich stars, the detection of H_2O came as a surprise. Past detections of SiO in carbon-rich stars (and HCN and CN detections in oxygen-rich stars) suggest that the difference in molecular abundances between carbon-rich and oxygen-rich stars is not a clear-cut one but only a general, albeit strong, trend (González-Delgado et al. 2003; Bieging et al. 2000; Bachiller et al. 1997; Bujarrabal et al. 1994; Olofsson et al. 1998). A confirmation of the presence of H_2O in IRC +10216 would be yet another challenge to the early dichotomized picture on molecular abundances in carbon-rich or oxygen-rich stars. Moreover, the presence of H_2O in IRC +10216 has potential implications beyond the scope of ordinary gas-phase chemistry. With additional detections of OH and H_2CO in IRC +10216 (Ford et al. 2003, 2004; Ford 2003), it has been suggested that these oxygen-based molecules in IRC +10216 are a result of swallowed and evaporated comets (Kuiper belt objects) as the old star expanded with age (Melnick et al. 2001; Ford et al. 2003; Ford & Neufeld 2001). A separate *Odin* observation of water in W Hydrae (an oxygen-rich star) yields a very high water abundance beyond the cosmic elemental oxygen abundance, suggestive of the same mechanism for water production in evolved stars (Justtanont et al. 2005). However, Willacy (2004) shows that H_2O and CH_4 can be generated in significant quantities through iron-nickel catalytic processes (Fischer-Tropsch catalysis), implying that the comet-evaporation scenario may not be the only explanation. With these new possibilities in scope, a confirmation observation of H_2O in IRC +10216 was urgently needed.

2. OBSERVATION

The *Odin* satellite is a joint astronomy-aeronomy mission under international collaboration between Sweden, Canada, France, and Finland.[3] It is equipped with a 1.1 m telescope, four

tunable submillimeter receivers, and one fixed-frequency receiver tuned to the 119 GHz ground-state transition of O_2 (Nordh et al. 2003; Frisk et al. 2003). The four submillimeter receivers span the frequency range of 480–580 GHz, allowing the satellite to observe many molecular lines not possible from the ground. Among the most important transitions are the 557 GHz ground-state rotation transition of ortho water and the 572 GHz ground-state transition of ortho ammonia.

The NH_3 observations were made with *Odin* between orbits 14765 and 14895 in 2003, November, toward IRC +10216. The total integration time including measurements at a sky reference position (see below) was 300 minutes. The target position for IRC +10216 was R.A. $= 09^h47^m57^s.2$ and decl. $= +13°16'44''.0$ (J2000.0), with an assumed local standard of rest stellar radial velocity (V_{LSR}) of -26.0 km s^{-1} (hereafter the systemic velocity). The phase lock and frequency stability of the 572 GHz receiver for the NH_3 ($J_K = 1_0 \rightarrow 0_0$, 572.4980678 GHz) line observation were checked by monitoring the telluric O_3 line ($J_{K^-,K^+} = 30_{4,26} \rightarrow 30_{3,27}$) at 572.8771486 GHz every orbit. The H_2O observations of IRC+10216 at 556.936 GHz ($J_{K^-,K^+} = 1_{10} \rightarrow 1_{01}$) were obtained with *Odin* between orbits 17426 and 17521 in 2004 May. The total integration time including measurements at a sky reference position was 440 minutes in the H_2O observing.

The observations were made in a position-switching mode, where the satellite was slewed in a 60 s switching cycle, to observe the target position and a sky reference position $+15'$ in R.A. from the target. At these submillimeter wavelengths, *Odin* has a beam size (FWHM) of $\sim 2'$. Pointing was better than $20''$ in both cases. Data were obtained using the 1024 channel acoustic-optical spectrometer (AOS) with a channel interval of 0.62 MHz (corresponding to 0.33 km s^{-1} at 556.936 GHz), giving a total frequency coverage of ~ 1 GHz. The data were processed and calibrated at the University of Calgary Space Astronomy Laboratory using the WinOdin software specifically developed for *Odin*. The averaged spectra were binned to a frequency resolution of 2.4748 MHz (velocity resolutions of 1.30 and 1.33 km s^{-1} at the NH_3 and H_2O frequencies, respectively). Twentieth-order polynomial baselines were subtracted from the averaged spectra. For comparison, sixth-order polynomial baselines were also used. There was no noticeable difference between the central sections $[-120$ km s$^{-1} < V_{LSR} - V_{LSR}$(source) $< +120$ km s$^{-1}]$ of the resultant spectra with the different orders of polynomial baselines.

Odin has a main beam efficiency (η_B) of 0.9. The internally calibrated intensity scale was expressed as the antenna temperature (T_A^*), but all intensity scales in this paper are expressed as the main beam brightness temperature (T_{MB}), where $T_{MB} = T_A^*/\eta_B$.

3. RESULTS

The final averaged *Odin* spectra of NH_3 and H_2O lines in IRC+10216 are shown in Figure 1 (without baseline removal) and Figure 2 (after baseline removal). The H_2O profile has a single-peak, round-top shape consistent with other molecular line spectra of IRC +10216 obtained with a large beam. The peak intensity T_{MB}(peak) is 0.060 ± 0.017 K at the frequency resolution of 2.5 MHz. The integrated intensity is 1.11 ± 0.11 K km s^{-1} for a velocity interval from -16 to $+16$ km s^{-1} with respect to the systemic velocity. The intensity of the *Odin* H_2O spectrum is consistent with that of the *SWAS* H_2O spectrum [T_A(peak) $= 0.02$ K; Melnick et al. 2001] if one takes into account the larger beam size of $3'.3 \times 4'.5$ and the main beam efficiency of 0.90 of *SWAS*.

The NH_3 spectrum has a peak intensity of 0.093 ± 0.023 K (2.5 MHz), an integrated intensity of 1.31 ± 0.15 K km s^{-1}, and a width of about 30 km s^{-1} at the detection limit. The width and the overall spectral shape of the NH_3 line are similar to those of
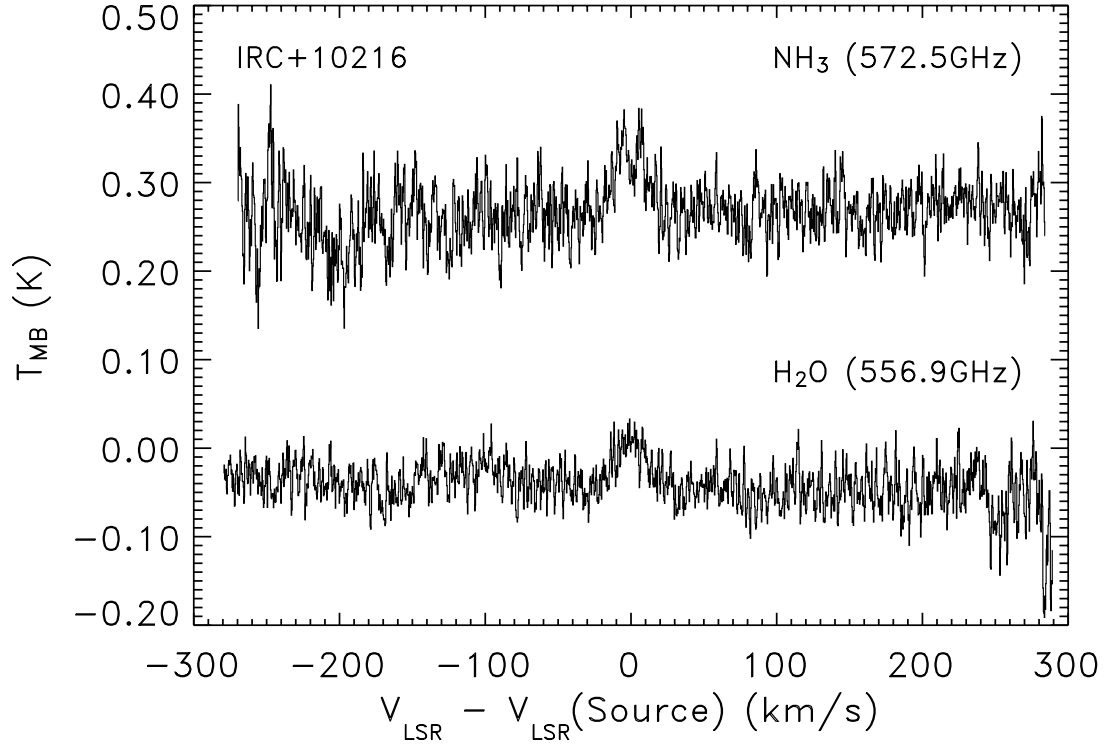
Fig. 1.—NH$_3$ ($J_K = 1_0 \rightarrow 0_0$) (*top*) and H$_2$O ($J_{K^-,K^+} = 1_{10} \rightarrow 1_{01}$) (*bottom*) spectra obtained with *Odin* in IRC +10216. The baselines have not been removed from the spectra. The frequency resolution is 0.62 MHz in this figure. The NH$_3$ spectrum has been offset by 0.35 K.
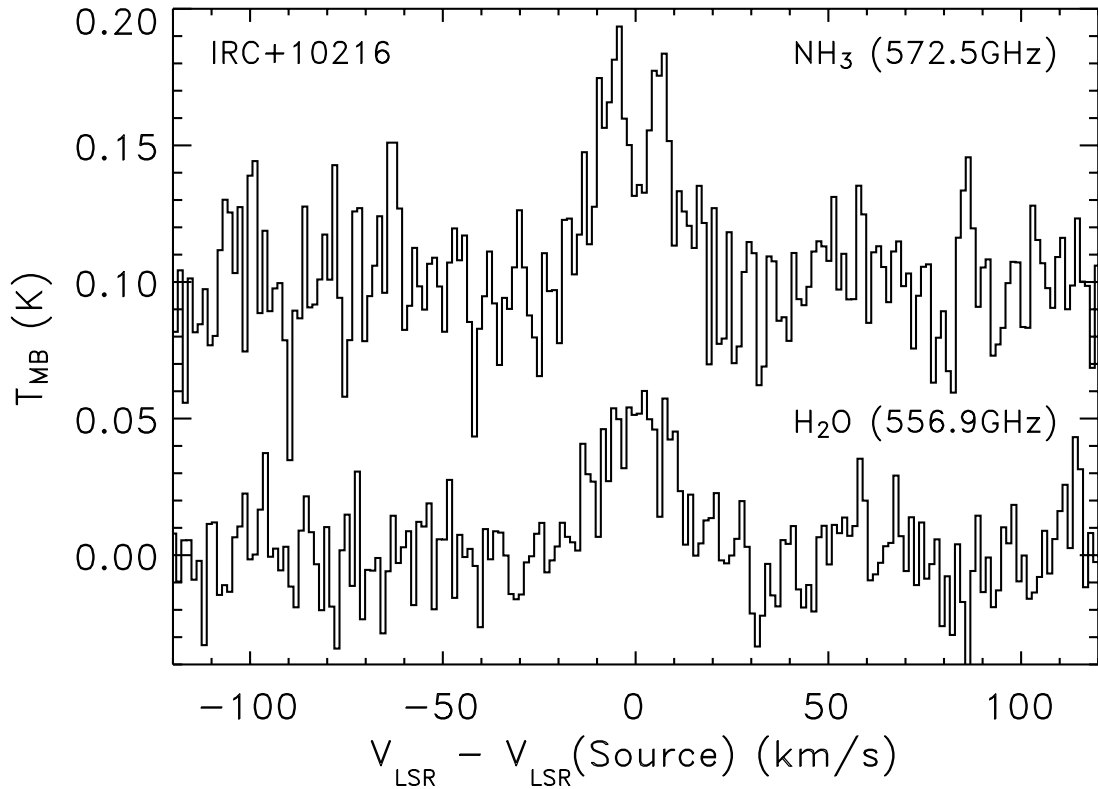

Fig. 2.—NH$_3$ ($J_K = 1_0 \rightarrow 0_0$) (*top*) and H$_2$O ($J_{K^-,K^+} = 1_{10} \rightarrow 1_{01}$) (*bottom*) spectra obtained with *Odin* in IRC +10216. The baselines have been removed. The frequency resolution is 2.5 MHz in this figure. The NH$_3$ spectrum has been offset by 0.1 K.
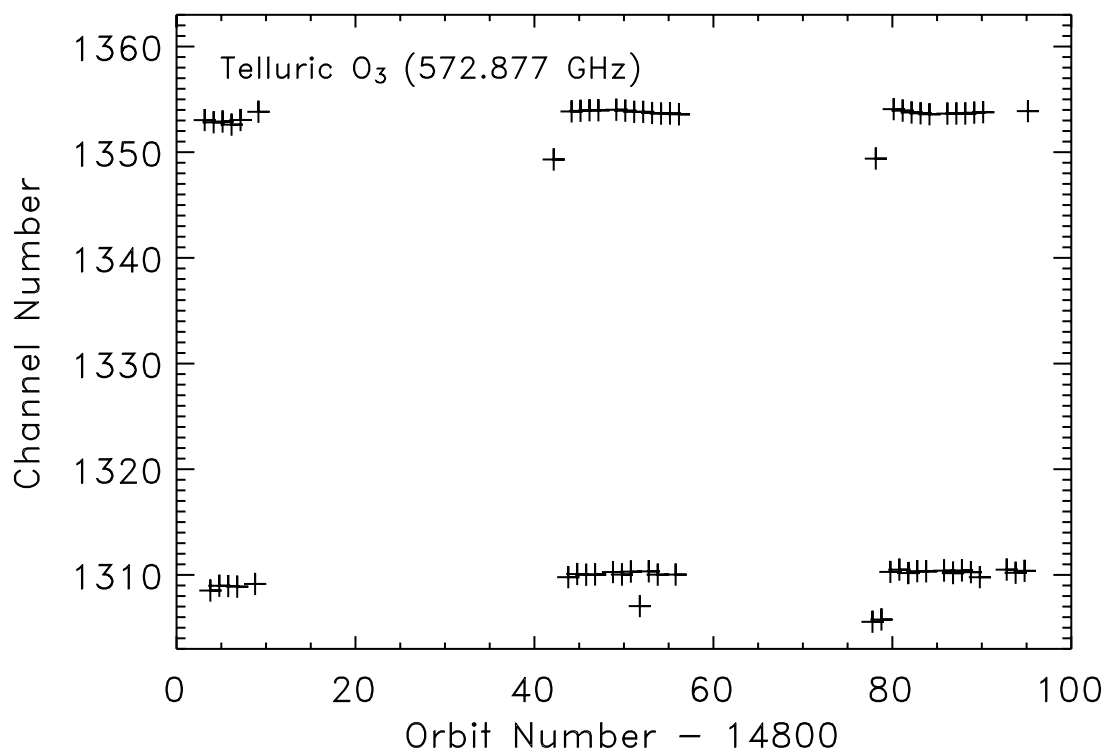
Fig. 3.—AOS channels onto which the telluric O_3 (572.877 GHz) line fell are plotted (*crosses*) with respect to the orbit number during the *Odin* NH_3 observation of IRC +10216. The upper group of points (blueshifted) correspond to the target rise seen from *Odin*, and the lower group of points (redshifted) correspond to the target set. The observations acquired during an orbit with a deviation of more than one channel from the average in the above plots were rejected before averaging. The channel interval is 0.62 MHz (0.32 km s^{-1}) in this figure.

H_2O and other molecular lines in IRC +10216. The present NH_3 profile, however, shows a depression at the systemic velocity ($V_{LSR} = -26$ km s^{-1}). Since the signal-to-noise ratio is only 4 for T_{MB}(peak) in the NH_3 spectrum, the observed profile may have simply been distorted by noise, and the actual profile may well be similar to that of H_2O. On the other hand, if the observed depression is real, then such a central depression is unusual for a molecular spectrum in an evolved star unless the emitting region is significantly larger than the beam size (which is unlikely).

The NH_3 (1_0–0_0) line consists of three hyperfine components (Townes & Schawlow 1955), but the hyperfine lines lie within 2 km s^{-1} in velocity, which is much smaller than the observed line width. Thus, the hyperfine lines should not affect the observed line shape and can be safely regarded as degenerate. Every effort was made to eliminate instrumental effects and distortions from the observation. Since the AOS was routinely used in H_2O and NH_3 observations by *Odin* at different times, the spectrometer should not be a cause of distortion. The stability of the local oscillator was checked by observing the telluric O_3 line every orbit. The observed O_3 profiles were inspected; their peak positions (determined with Gaussian fitting) in spectrometer channel are plotted as a function of orbit number in Figure 3. After inspection and rejection of bad data, we include only reliable data in the averaged NH_3 spectrum in Figure 2. Since absorption by cooler outer parts of the molecular envelope should appear at a velocity significantly blueshifted from the systemic velocity, absorption within the expanding envelope is ruled out as a cause for the depression at the systemic velocity. One possible explanation for a double peak profile is an unresolved torus (or a disk). Ford et al. (2003), in their attempt to interpret their OH spectrum, suggest such a geometry and present a model double-peaked profile. Given the low signal-to-noise level of our NH_3 spectrum, how-

ever, an exploration of such a possibility should wait another, better quality NH_3 spectrum.

4. ANALYSIS

Model profiles were fitted to the observed spectra of NH_3 and H_2O. The model profiles were calculated with excitation and radiative-transfer codes for NH_3 and H_2O. Both of the NH_3 and H_2O codes employ the large velocity gradient (LVG) algorithm (or Sobolev approximation) in a spherically symmetric geometry for radiative transfer calculations (Deguchi & Nguyen-Q-Rieu 1990). We assumed a constant radial expansion for the model envelope. Local line broadening with a width of 1 km s^{-1} (FWHM) was taken into account when a model profile was calculated. We included, in the excitation calculations, IR illumination from a central star that was approximated as a blackbody with an assumed radius and an assumed surface temperature, consistent with an assumed luminosity of the model central star. Local IR radiation from dust within the molecular envelope was not considered in the present work.

The ortho-H_2O (o-H_2O) excitation calculations include the $(\nu_1, \nu_2, \nu_3) = (0, 0, 0)$ (ground state), (0, 1, 0) (first excited bending mode), and (0, 0, 1) (antisymmetric O-H stretch) vibrational states with 61 rotational levels in each vibrational state. The ortho-NH_3 (o-NH_3) excitation calculations only included the $K = 0$ ladder ($J = 0$ through 11) of o-NH_3 in the ground vibrational state. The omission of the $K = 3n$ ($n \geq 1$) levels should not significantly affect the excitation analysis of the $J_K = 1_0 \rightarrow 0_0$ line. The $K = 3n$ ($n \geq 1$) levels interact with the $K = 0$ levels only through collisional transitions. The $J_K = 3_3$ level, the lowest of the omitted o-NH_3 levels, is higher than the $J_K = 2_0$ level in excitation energy. Thus, the inclusion of the $K = 3n$ ($n \geq 1$) levels will have an effect on the excitation of the $J_K = 1_0 \rightarrow 0_0$

TABLE 1
MODEL PARAMETERS

Parameters	Value
Distance D	130 pc
Expansion velocity V_e	15.0 km s^{-1}
Inner boundary R_1	1.33×10^{15} cm
Outer boundary R_2	4.01×10^{16} cm
Density $n_1(H_2)$ at R_1	$8.11 \times 10^{+6}$ cm^{-3}
Gas temperature T_1 at R_1	500 K
Density distribution $n_r(H_2)$.................	$n_1(H_2)\,(r/R_1)^{-2}$
Temperature law T_r............................	$T_1(r/R_1)^{-0.7}$
Mass-loss rate $\dot{M}$	$1.43 \times 10^{-5}\,(1+4f_{He})\,M_\odot$ yr^{-1}[a]
Stellar temperature (photosphere)	2000 K
Stellar luminosity..................................	9600 $L_\odot$
Star radius R_{star}	5.68×10^{13} cm (3.79 AU)

Derived Abundance	
$X(o\text{-}NH_3)$[b].............................	6.3×10^{-7}
$X(o\text{-}H_2O)$.............................	2.4×10^{-6}

[a] f_{He} is the relative abundance of He to H.
[b] Underestimated by $\sim$30%–50% (see text).

transition similar to one in which the statistical weights of the $J \geq 2$ ($K = 0$) levels are artificially increased. Collisional rates were taken from Green et al. (1993) for H$_2$O-He (converted to H$_2$O-H$_2$) and from Danby et al. (1988) for NH$_3$-H$_2$ (para). The collisional rates from Danby et al. (1988) were used for both ortho and para forms of H$_2$.

The physical parameters such as mass-loss rate, expansion velocity, etc., are taken from Men'shchikov et al. (2001) and Schöier et al. (2002). The density and temperature profiles in the CSE are assumed to have power-law distributions. A constant mass-loss rate is assumed in the present model. The radial thick-

ness (common to NH$_3$ and H$_2$O) of the model CSE is defined by the inner boundary R_1 and the outer cutoff R_2. The inner boundary is estimated from Monnier et al. (2000) and Keady & Ridgway (1993). Monnier et al. (2000) categorically reject the presence of a significant amount of NH$_3$ for $r < 1.3 \times 10^{15}$ cm and $T_k > 500$ K, where r and T_k are the radius and the gas temperature, respectively. The outer cutoff is adopted from Nguyen-Q-Rieu et al. (1984). The only free parameter remaining in the profile fitting is the (radially constant) relative abundance $X(o\text{-}H_2O)$ or $X(o\text{-}NH_3)$. The adopted parameter values and the best-fit $X(o\text{-}NH_3)$ and $X(o\text{-}H_2O)$ values are summarized in Table 1.

The best-fit spectral line profiles are shown in Figure 4. Although the model gives an excellent fit to the observed profile of H$_2$O, the fit to the NH$_3$ profile is less satisfactory. Unless the assumed density $n_1(H_2)$ is very high (of the order of 2×10^8 cm^{-3} or higher, corresponding to a mass-loss rate of $\sim 4 \times 10^{-4}$ $M_\odot$ yr^{-1} or higher), a model profile with a flat top or a central depression cannot be generated for a source smaller than the beam size.

In the best-fit models, the ground rotational transitions of o-NH$_3$ and o-H$_2$O are both subthermally excited. The T_{ex}/T_k ratio is 108/500 K at the inner boundary for the 1_{10}–1_{01} transition of o-H$_2$O. The corresponding ratio for the 1_0–0_0 transition of o-NH$_3$ is 115/500 K. The T_{ex}/T_k ratio drops to 0.1 or much lower in the outer regions for both of the transitions. Since collisional deexcitation is insignificant in the best-fit models, the estimated abundances from the present models are dependent on the adopted collisional excitation rates and the assumed IR radiation field.

From the integrated line strengths, we can derive the abundances of H$_2$O and NH$_3$ relative to H$_2$. These derived abundance values scale approximately as $X \propto \dot{M}^{-2}D^2$, where D is the assumed distance to IRC +10216. Assuming a distance of 130 pc and a mass-loss rate of $\dot{M} = 1.4 \times 10^{-5}$ $M_\odot$ yr^{-1}, we obtain a relative abundance of 2.4×10^{-6} for o-H$_2$O in IRC +10216. Our result from the *Odin* observation is consistent with the abundance
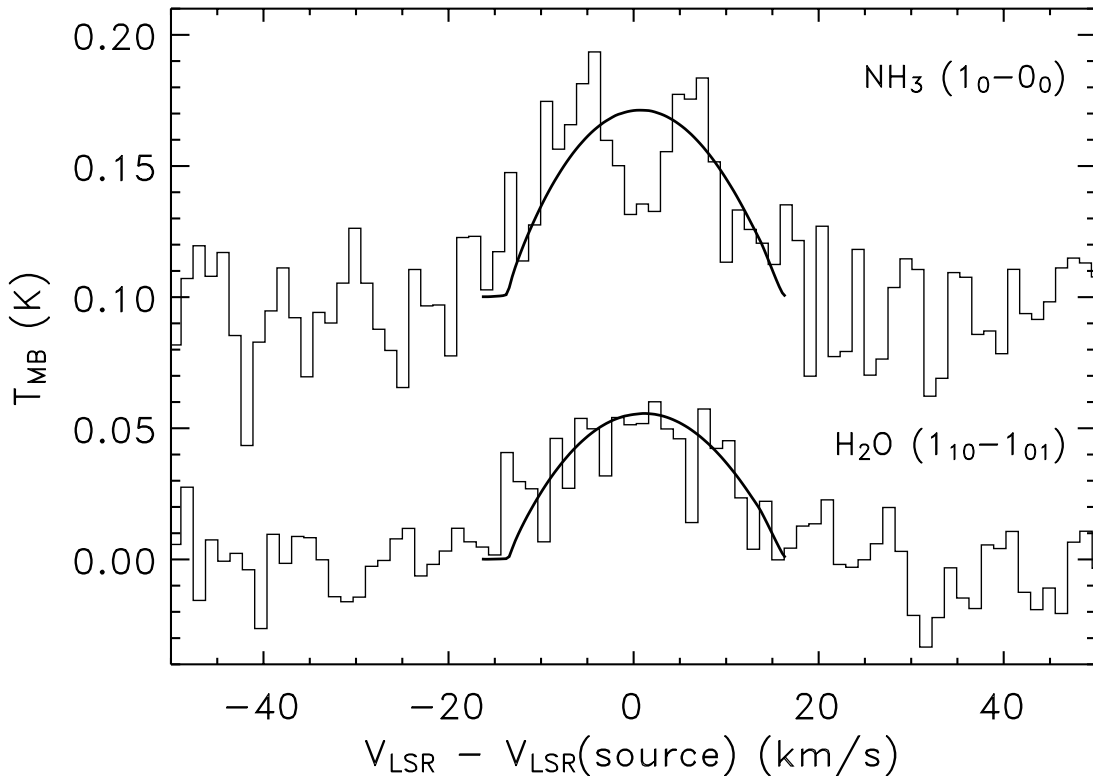

FIG. 4.—Model NH$_3$ and H$_2$O spectra of IRC+10216 (*thick lines*) plotted together with the observed spectra (*histograms*).

of 2.5×10^{-6} (at 170 pc with $\dot{M} = 2.0 \times 10^{-5}\ M_\odot\ \mathrm{yr}^{-1}$) from the *SWAS* observation (Melnick et al. 2001). The H_2O abundance is comparable to those of CH_4, CS, CCH, and CN in IRC +10216 (cf. Table 1 in Glassgold 1996).

The derived abundance for o-NH_3 is 6.3×10^{-7}. Since our NH_3 excitation code includes only the $K = 0$ rotational states, and X(o-NH_3) in Table 1 is underestimated by 30%–50%, we estimate that the actual abundance of o-NH_3 is 1×10^{-6}. This value is significantly higher than 3×10^{-8} for para-NH_3 derived from the 24 GHz observations (Nguyen-Q-Rieu et al. 1984; Kwok et al. 1981). Abundance estimates for NH_3 (ortho and para) from IR observations range from 2×10^{-7} to 8×10^{-7} (Betz et al. 1979; Keady & Ridgway 1993; Monnier et al. 2000). An accuracy in mass-loss rate of $\pm 50\%$ propagates to a range of $(0.5-2) \times 10^{-6}$ for the (o-NH_3) abundance estimate in the present work. Given these uncertainties in the abundance estimate, the present estimate is in line with those from IR observations. The IR absorption spectra in Keady & Ridgway (1993) show no hint of an abundance disparity of order 30 between the ortho- and para-NH_3. The difference between the 24 GHz and present results appears to reflect the difference in excitation requirements (and hence difference in probed gas volume). The present o-NH_3 abundance estimate has a very weak dependence on R_2 (the outer boundary). If the R_2 value is twice the value in Table 1, X(o-NH_3) decreases by only 3%. If the R_2 value is half the value in Table 1, X(o-NH_3) increases by only 8%. Thus, if X(o-NH_3) dramatically decreases from 1×10^{-6} to 3×10^{-8} outward for $r > 2 \times 10^{16}$ cm [$n(H_2) < 3.5 \times 10^4\ \mathrm{cm}^{-3}$], the present X(o-NH_3) estimate approximately stands. Meanwhile, the thermalization density for the 24 GHz transitions is about $10^4\ \mathrm{cm}^{-3}$, and the 24 GHz lines can easily be excited in the outer part ($r > 2 \times 10^{16}$ cm), where the gas temperature is 50–80 K in the model in Table 1.

5. DISCUSSION

The present *Odin* observation of the H_2O line eliminates any doubt about the *SWAS* detection of this molecule and firmly establishes the presence of a significant amount of water vapor in the CSE of this carbon-rich late-AGB star. Since the conventional (LTE and non-LTE) gas-phase chemical models all fail to predict the presence of H_2O, Melnick et al. (2001) have proposed a scenario in which Kuiper belt objects (comets) are vaporized in the CSE. While this is a very exciting hypothesis, other formation processes such as grain-related processes need to be explored.

Willacy (2004), for example, has shown that under certain conditions, the Fischer-Tropsch (F-T) catalytic processes are able to generate H_2O and CH_4 in sufficient quantities to explain observed H_2O in IRC +10216. The high abundance of H_2O also leads to a detectable amount of OH through photodissociation of H_2O. The proposed F-T mechanism was first employed to explain the observed molecular abundances in the solar nebula during the planet formation (including the pristine comet composition; Kress & Tielens 2001). It would therefore be difficult to differentiate the formations of H_2O and CH_4 through the F-T catalysis during the AGB mass-loss phase from the evaporation of H_2O and CH_4 from comets the composition of which is explained by the F-T process during the pre–main-sequence phase. The weakness with the F-T based model is that the F-T process possibly produces alkanes, alkenes, carbon dioxide, and alcohols, in particular, as well as water and methane (Willacy 2004), but a sensitive search for CH_3OH has set a strong upper limit to CH_3OH abundance ($CH_3OH/H_2O < 7.7 \times 10^{-4}$) (Ford et al. 2004). A future F-T model will need to explicitly include the

(thus far omitted) CH_3OH production channel and yet satisfy the observational constraint on the CH_3OH abundance.

The present estimate of 1×10^{-6} for NH_3/H_2 in IRC +10216 reiterates another challenge to chemical models. The LTE chemical models for the atmosphere of a carbon-rich star all predict $X(NH_3)$ less than 1×10^{-10} at $P/k = n(H_2)\,T = 4.8 \times 10^{16}\ \mathrm{K\ cm}^{-3}$ for elemental abundance C/O = 1.1−3.5 (Cherchneff & Barker 1992). The only case in Cherchneff & Barker (1992) in which $X(NH_3)$ is as high as 1×10^{-7} is under the extreme condition $T = 1008$ K and $n(H_2) = 4.8 \times 10^{16}\ \mathrm{cm}^{-3}$.

In non-LTE gas-phase chemical models, NH_3 is in most cases either assumed to be initially present (Millar & Herbst 1994) or not considered at all (Cherchneff et al. 1993; Glassgold et al. 1986; Glassgold 1996). Nejad & Millar (1987) and Millar & Herbst (1994 and references therein) assume a high abundance of NH_3 ($NH_3/H_2 = 2 \times 10^{-6}$) as an initial condition at the inner boundary of the model CSE together with $X(CO) = 1 \times 10^{-4}$, $X(C_2H_2) = 2 \times 10^{-5}$, $X(HCN) = 6 \times 10^{-6}$, $X(CH_4) = 2 \times 10^{-6}$, and $X(N_2) = 1.84 \times 10^{-5}$. With these initial (inner boundary at $r = 1 \times 10^{16}$ cm) conditions, the NH_3/H_2 ratio remains at 5×10^{-7} for $r < 6 \times 10^{16}$ cm, beyond which NH_3/H_2 drops drastically below 1×10^{-10} at $r = 2 \times 10^{17}$ cm as a result of photo-dissociation without net formation. The present work supports the high initial values of NH_3 abundance assumed in the models by Millar and collaborators, but the origin of such high abundance is still unexplained. From the infrared absorption studies, Keady & Ridgway (1993) suggest that most of the IR absorption by NH_3 occurs near $r = 3 \times 10^{16}$ cm.

Willacy & Cherchneff (1998) considered a shock chemistry in addition to the usual quiescent gas chemistry in the outward-moving gas. Although NH_3 is considered in their model, NH_3 is not generated in abundance in the model. They suggest a possibility (also suggested by Keady and Ridgway 1993) that these simple hydrogenated species are ejected when gas molecules condense into grains. The possibility that grain surface reactions may be responsible was proposed by Lafont et al. (1982). For example, H atoms may be adsorbed or directly react with grain surface materials, and carbonaceous grain surfaces may generate CH_4 in the gas phase. These possibilities should be explored more specifically and quantitatively.

In comparison with H_2O and CH_4, the present estimate for NH_3 abundance is significantly higher in IRC +10216 than in comets in the solar system. The NH_3/H_2O ratio in IRC +10216 is about 0.4 in the present work. The observed NH_3/H_2O ratios in comets are about 0.007 (Hale-Bopp), 0.004 (Hyakutake), and 0.01 (1P/Halley) (Iro et al. 2003; Bockelée-Morvan et al. 2000). If these low ratios apply to all Kuiper belt objects, the evaporation of comets may not be sufficient to explain the observed NH_3/H_2O ratio in IRC +10216. In addition, there is a growing body of evidence for a strong depletion of elemental nitrogen in comets, and the low NH_3 and N_2 abundances (relative to H_2O in particular) seem widespread among comets (Iro et al. 2003). The extrasolar comets may have very different chemical compositions, however. Meanwhile, it is not clear whether the Fischer-Tropsch (or a similar) process enhances the abundance of NH_3. There have been suggestions that NH_3 may be formed from N_2 through a process similar to Fischer-Tropsch catalysis in the solar nebula (Kress & Tielens 2001). While the N_2 dissociation process may be difficult to happen, an experiment is highly desirable (Kress & Tielens 2001). Theoretical studies incorporating an enhanced production of NH_3 through Fischer-Tropsch catalysis or similar catalytic processes would substantially advance our

understanding of the origin of NH$_3$ and H$_2$O in carbon-rich AGB stars.

6. CONCLUSIONS

We have detected the ground-state rotational transitions of water and ammonia in the circumstellar envelope of IRC+10216 and derived their relative abundances from line-transfer models. The high abundances of both ammonia and water is a mystery as current LTE and non-LTE gas-phase chemistry models have failed to produce the observed abundance. While the hypothesis of comet vaporization is very attractive in explaining the origin of water in IRC+10216, it does not account for the equally high abundance of ammonia. These results show that our theoretical understanding of circumstellar chemistry is rudimentary, and some (unspecified) fundamental processes are still missing in the models.

REFERENCES

Bachiller, R., Fuente, A., Bujarrabal, V., Colomer, F., Loup, C., Omont, A., & de Jong, T. 1997, A&A, 319, 235
Bell, M. B., Kwok, S., Matthews, H. E., & Feldman, P. A. 1982, AJ, 87, 404
Betz, A. L., McLaren, R. A., & Spears, D. L. 1979, ApJ, 229, L97
Bieging, J. H., Shaked, S, & Gensheimer, P. D. 2000, ApJ, 543, 897
Bockelée-Morvan, D., et al. 2000, A&A, 353, 1101
Bujarrabal, V., Fuente, A., & Omont, A. 1994, A&A, 285, 247
Cherchneff, I., & Barker, J. R. 1992, ApJ, 394, 703
Cherchneff, I., Glassgold, A. E., & Mamon, G. A. 1993, ApJ, 410, 188
Danby, G., Flower, D. R., Valiron, P., Schilke, P., & Walmsley, C. M. 1988, MNRAS, 235, 229
Deguchi, S., & Nguyen-Q-Rieu 1990, ApJ, 360, L27
Ford, K. E. S. 2003, BAAS, 34, 12.63
Ford, K. E. S., & Neufeld, D. A. 2001, ApJ, 557, L113
Ford, K. E. S., Neufeld, D. A., Goldsmith, P. F., & Melnick, G. J. 2003, ApJ, 589, 430
Ford, K. E. S., Neufeld, D. A., Schilke, P., & Melnick, G. J. 2004, ApJ, 614, 990
Frisk, U., et al. 2003, A&A, 402, L27
Glassgold, A. E. 1996, ARA&A, 34, 241
Glassgold, A. E., Lucas, R., & Omont, A. 1986, A&A, 157, 35
González-Delgado, D., Olofsson, H., Kerschbaum, F., Schöier, F. L., Lindqvist, M., & Groenewegen, M. A. T. 2003, A&A, 411, 123
Green, S., Maluendes, S., & McLean, A. D. 1993, ApJS, 85, 181
Iro, N., Gautier, D., Hersant, F., Bockelée-Morvan, D., & Lunine, J. I. 2003, Icarus, 161, 511

Justtanont, K., et al. 2005, A&A, 439, 627
Keady, J. J., & Ridgway, S. T. 1993, ApJ, 406, 199
Kress, M. E., & Tielens, A. G. G. M. 2001, Meteoritics Planet. Sci., 36, 75
Kwok, S., Bell, M. B., & Feldman, P. A. 1981, ApJ, 247, 125
Lafont, S., Lucas, R., & Omont, A. 1982, A&A, 106, 201
Melnick, G. J., Neufeld, D. A., Ford, K. E. S., Hollenbach, D. J., & Ashby, M. L. N. 2001, Nature, 412, 160
Men'shchikov, A. B., Balega, Y., Blöcker, T., Osterbart, R., & Weigelt, G. 2001, A&A, 368, 497
Menten, K. M., & Alcolea, J. 1995, ApJ, 448, 416
Millar, T. J., & Herbst, E. 1994, A&A, 288, 561
Monnier, J. D., Danchi, W. C., Hale, D. S., Tuthill, P. G., & Townes, C. H. 2000, ApJ, 543, 868
Nejad, L. A. M., & Millar, T. J. 1987, A&A, 183, 279
Nguyen-Q-Rieu, Graham, D., & Bujarrabal, V. 1984, A&A, 138, L5
Nordh, H. L., et al. 2003, A&A, 402, L21
Olofsson, H. 1999, in IAU Symp. 191, Asymptotic Giant Branch Stars, ed. T. Le Bertre, A. Lebre, & C. Waelkens (San Francisco: ASP), 3
Olofsson, H., Lindqvist, M., Nyman, L.-Å., & Winnberg, A. 1998, A&A, 329, 1059
Schöier, F. L., Ryde, N., & Olofsson, H. 2002, A&A, 391, 577
Townes, C. H., & Schawlow, A. L. 1955, Microwave Spectroscopy (New York: McGraw-Hill)
Tsuji, T. 1964, Ann. Tokyo Astron. Obs., 2nd Ser., 9, 1
Willacy, K. 2004, ApJ, 600, L87
Willacy, K., & Cherchneff, I. 1998, A&A, 330, 676